

Strain Dependence of the Viscoelastic Properties of Alginate Hydrogels

Rebecca E. Webber and Kenneth R. Shull*

Department of Materials Science and Engineering, Northwestern University, 2220 Campus Dr., Evanston, Illinois 60208-3108

Received April 14, 2004; Revised Manuscript Received June 4, 2004

ABSTRACT: Alginates, naturally derived linear copolymers of 1,4-linked β -D-mannuronic acid and α -L-guluronic acid residues, can form hydrogels in the presence of divalent cations. In this study alginate hydrogels were formed by the addition of Ca^{2+} ions to aqueous solutions of sodium alginate. The rheological and mechanical behaviors of the hydrogels were studied using an axisymmetric probe tack apparatus with stress relaxation and cyclic movement capabilities. The hydrogels were subjected to high compressive strains (several units) to elucidate the source of nonelastic stress relaxation. These polysaccharide hydrogels behave elastically at small strains and become viscoelastic at large strains, a result that is responsible for the excellent toughness of the gels.

Introduction

Transient networks, polymer gels in which the physical cross-links can be broken and recovered, have been of recent interest to the scientific community, especially due to their potential as soft, dissipative materials for biomedical applications.^{1–3} Examples of soft networks in bioapplications include protein-based hydrogels, self-assembling amphiphilic polymers, gelatin, and ionic alginate hydrogels.^{4–13} Uses for these materials include injectable drug delivery systems, scaffolds for tissue engineering, and cell encapsulation and transplantation.^{4,5,9,13–15}

Alginates are naturally derived linear copolymers of 1,4-linked β -D-mannuronic acid and α -L-guluronic acid residues.^{6,13,16} The structure of this copolymer is shown in Figure 1. The β -D-mannuronic acid (M) residues and the α -L-guluronic acid (G) residues vary in proportion and sequential distribution along the length of the alginate chain, depending on the organism (primarily several species of brown kelp) from which the alginate is isolated.^{8,13,16} There is no regular repeat unit in alginate polymers, and the chains can be envisioned as a varying sequence of regions termed M blocks, G blocks, or MG blocks (predominantly alternating M and G residues), named according to their acid residue content.^{13,16} These polysaccharides form hydrogels in the presence of divalent ions via an ionic interaction between the acid groups on the G blocks and the chelating ions, generally Ca^{2+} .^{4,17} As a result, alginate gels are physically cross-linked systems with mechanical properties dependent on the proportion and length of the G blocks in a given alginate chain.^{6,13} It is thought that the calcium ions only bind between G blocks of greater than 20 units, and at high calcium concentrations, cross-linking between multiple G blocks is possible.^{18–20} The gels are viscoelastic solids, with a network structure described by the “egg-box” model.^{17,20,21} The modulus of ionic alginate gels depends on the molecular weight of the alginate copolymer, the composition and sequence of the copolymer, and the cation used in gelation.^{6,20,22} Alginate hydrogels are used for a variety of bioapplications including immobilizing living cells, cell encapsulation and transplantation, immobilization of enzymes, and drug and protein delivery.^{6,8,9,13,23–25} Additionally, alginate is a suitable material for tissue engineering

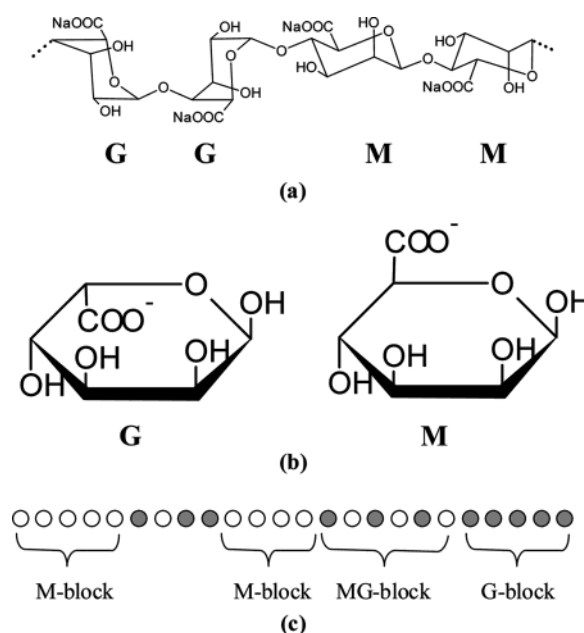


Figure 1. (a) Compositional structure of sodium alginate, (b) structures of the α -L-guluronic acid (G) and β -D-mannuronic acid (M) residues of which it is composed, and (c) schematic representation of the residue sequence.

applications as it is considered biocompatible and is resistant to protein absorption.^{4,14,15} Alginates are also commonly used as food additive gelling agents.^{16,26}

The mechanical and rheological properties of many varieties of alginate gels have been investigated as well as the effect of environment and ionic species on these properties.^{6,18,20,22,24,27,28} Rheological studies have often focused on the change in modulus during the sol–gel transition in alginate hydrogels.^{20,22,26,28,29} These materials are generally found to behave elastically after complete gelation, with moduli on the order of 1 kPa to several hundred kPa.^{20,22,26,28,29} Additionally, groups have studied alginate gel stability over time in the presence of various divalent and monovalent cations and in a physiological environment.^{6,24,30}

Despite the large body of work that has been done on these materials, the origin of elasticity in alginate hydrogels, as in most transient networks, is not com-

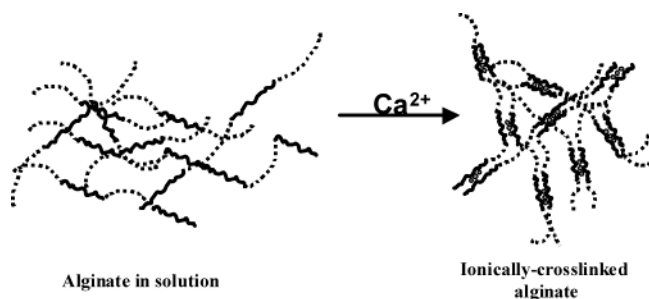


Figure 2. Ionic cross-linking and gelation in sodium alginate. Many Ca^{2+} ions participate in each junction.

pletely understood. The general theory of rubber elasticity is inapplicable to these materials because alginate chains do not exhibit the random-coil behavior assumed by the theory and because of the nature of the physical cross-links.^{22,28,31} Alginate gels have long junction zones of ion complexation rather than discrete, pointlike cross-links, as shown schematically in Figure 2.^{18,19,22} The lengths of these junctions are presumed to be responsible for the unique mechanical response of alginate hydrogels, including their high fracture toughness.¹⁸ Ionically cross-linked alginate gels are considered non-equilibrium systems with behavior governed by kinetics rather than thermodynamics.^{22,28} Their moduli exhibit complex temperature-dependent behavior that does not coincide with thermodynamic considerations.²² Further, the viscoelastic behavior of alginate hydrogels is evidence of kinetic effects in a nonequilibrium, nonelastic system; these are not truly elastic materials. However, alginate gels often exhibit elastic behavior at low strains, where the frequency dependence of the dynamic moduli can be quite small.^{22,28}

In this study we investigate the viscoelastic behavior of highly cross-linked ionic alginate hydrogels using an axisymmetric probe tack apparatus. This device is capable of performing both stress relaxation and oscillatory experiments. Using these techniques, we focus specifically on the effect of strain amplitude on the mechanical response and elastic modulus of the gels. We are mainly interested in high strain response (as high as several strain units), motivated by the fact that high strain deformation mechanisms are largely responsible for the toughness exhibited by transient gel systems, especially when compared with covalently cross-linked gel networks.¹⁸ These experiments are performed in compression because of the test simplicity and because of the need to avoid fracture of the hydrogels during testing.

Methods

The alginate gels used in these investigations are made from Protanal LF 200 DL sodium alginate from FMC Biopolymer. The structure of this alginate is 55–65% guluronic acid and 35–45% mannuronic acid. The molecular weight is estimated to be 270 000–320 000 g/mol from viscosity measurements, giving 200–400 mPa·s (for 1% aqueous solutions).³² This particular material is generally used in dental impression materials and for sustained release applications. The alginate gel is formed from a 2% (w/w) solution of the sodium alginate in water. All water used in this investigation was deionized by a Nanopure filtration system to a resistivity of 18 M Ω ·cm. To create a physiological buffer and slow down the gelation process, 8 g/L of sodium chloride (NaCl) and 4 g/L of sodium metaphosphate ($\text{Na}(\text{PO}_3)_6$) are added to the aqueous sodium alginate solution. The resulting suspension is mixed for a minimum of 8 h. A supersaturated aqueous solution of calcium

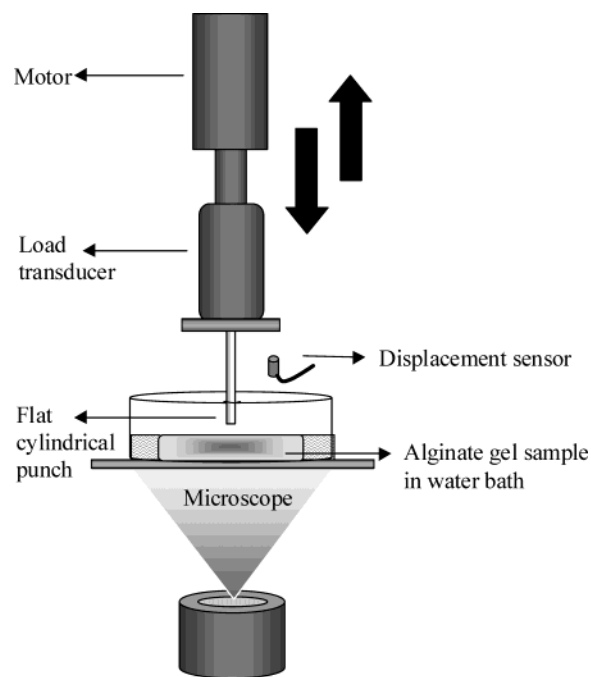


Figure 3. Schematic of the axisymmetric probe tack apparatus.

sulfate (CaSO_4) (210 g/L) is added to the alginate suspension by using two 3 mL syringes coupled by a double luer connector, allowing vigorous mixing to achieve a homogeneous solution. The volume ratio of alginate to calcium sulfate solutions is 30:1. This mixture is poured between two heavy glass plates separated by shims of variable thickness. Gelation occurs within 5 min after the addition of the calcium solution. This procedure creates flat, uniform gels of desired thickness. The gel thickness used in these studies is 2 mm. To allow excess calcium to leach out, the gel is soaked in a water bath for a minimum of 24 h. This method uses a 1:1 molar ratio of G units to calcium ions, which is sufficient for rapid, complete gelation. Similar procedures have been used in the literature,^{6,8,14,15} and many studies have been performed to determine the compositions and gel-making procedures (i.e., concentration of the chelating and cross-linking ions, mixing methods) that produce optimal alginate gel properties for various applications.^{6,8,24,26} For our purposes, the simplistic gel procedure used produced consistent results, and further optimization was unnecessary.

The rheological and mechanical tests were performed on an axisymmetric probe tack device, shown in Figure 3. The general test method, described in detail elsewhere, entails bringing a rigid cylindrical punch into contact with the surface of the hydrogel using a piezoelectric stepping motor.^{33–35} Load and displacement data are collected through a load transducer and optical displacement sensor during compression of the gel. The radius of the punch (a_0) used in these tests was 390 μm . Tests were conducted in a dish containing a shallow level of deionized water to prevent gel dehydration. However, stress relaxation tests performed in air (not included in this work) gave comparable results, and low-strain relaxed sine wave test results were indistinguishable when tested in air and water. Additionally, from repeated stress relaxation and relaxed sine wave tests it was determined that aging of the gel in a saturated water environment over the course of 5 months did not affect the mechanical properties, although previously published work implies that eventual degradation of the properties may be inevitable.¹⁵

Stress relaxation tests were performed by compressing the gel to a specified maximum load and then holding the resulting displacement constant while the load was allowed to relax over a predetermined period of time. Relaxed sine wave tests, consisting of a stress relaxation experiment followed immediately by an oscillatory test, allowed measurement of the

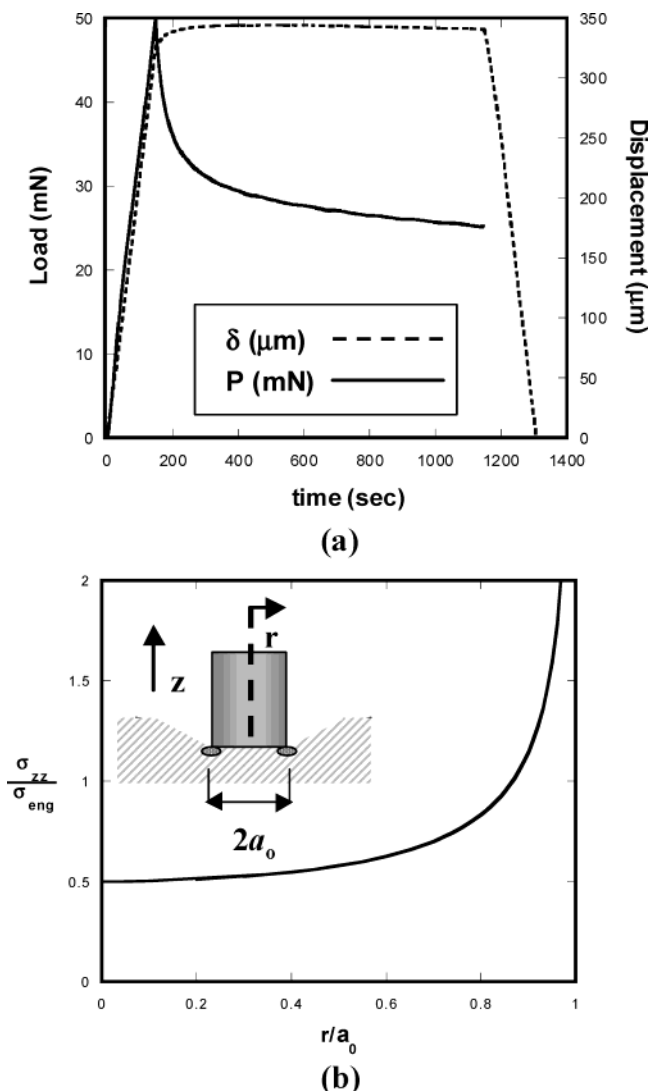


Figure 4. (a) Load and displacement data as a function of time during a typical stress relaxation experiment ($P_{\max} = 50$ mN). (b) Stress distribution under a flat cylindrical punch in contact with an elastic half-space normalized by the average engineering stress and plotted as a function of the radial distance from the center of the punch. The inset schematic defines the plot parameters and illustrates the stress singularity that exists at the contact edge.

bulk rheology of the samples. The oscillatory portion of the test entails imposing a small-strain displacement amplitude on the sample at various frequencies as the load is recorded. The tests were performed over a frequency range of 0.01–1 Hz. Because of the test geometry, the contact area between the probe and the thin gel remains constant after initial contact. In this case, the complex modulus can be calculated from the relative magnitudes of the sinusoidal load and displacement curves and from the phase lag between them. The oscillatory test method has been described in detail elsewhere, and results from these tests have been shown to be consistent with conventional rheological measurements.³⁶

The load (P) and displacement (δ) data for a typical stress relaxation experiment are shown in Figure 4a. It can be seen that the maximum compressive displacement is maintained at a constant value (δ_{\max}) while the load is monitored to discern stress relaxation within the gel. During a compressive test, the strains in the system are determined by the normalized displacement, δ/a_0 .³⁷ Although strain in axisymmetric probe tests on thin polymer layers is often represented as δ/h where h is the layer thickness, the quantity δ/a_0 is more appropriate for these experiments because the gel layers are thick.^{35,38} As the layer thickness approaches infinity, becoming effectively

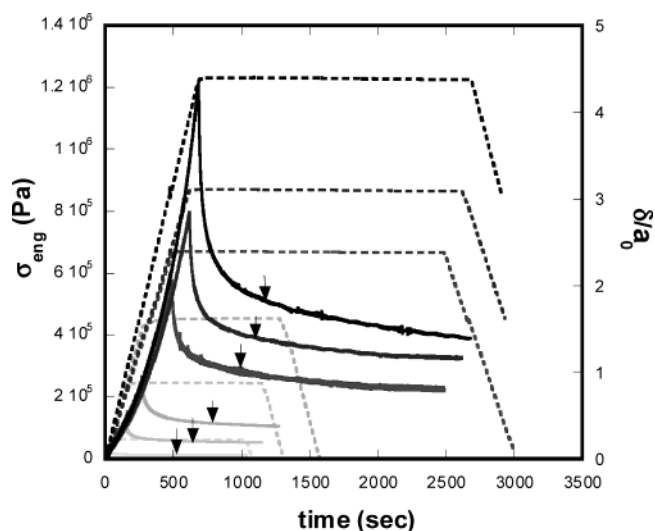


Figure 5. Stress (solid lines) and normalized displacement (dotted lines) curves as a function of time during a typical stress relaxation experiment. Maximum compressive displacements were $0.23a_0$, $0.89a_0$, $1.62a_0$, $2.38a_0$, $3.10a_0$, and $4.38a_0$. The arrow on each of the stress curves represents the time at 500 s after δ_{\max} was attained. These stress values were used to determine the moduli plotted in Figure 7.

an elastic half-space, h loses significance and a_0 is the only relevant length scale in the problem. The quantity δ/a_0 therefore specifies the overall state of strain in the gel.

To further understand stress and strain in this soft hydrogel, it is useful to consider the load–displacement relationship for elastic materials. For small compressive strains, the load is linearly related to the displacement through the compliance of the layer, which is given by $C_0 = \delta/P = 3/(8Ea_0)$ for a flat, cylindrical punch in contact with an incompressible elastic half-space with an elastic modulus E .³⁷ This equation assumes a rigid, frictionless punch engaged in adhesionless contact with a thick layer having a Poisson's ratio of 0.5.³⁷ We can also define an average engineering stress for this problem, given by $\sigma_{\text{eng}} = P/(\pi a_0^2)$. When coupled with the compliance, this equation leads to the following expression for σ_{eng} :

$$\frac{\sigma_{\text{eng}}}{E} = \frac{8}{3\pi} \frac{\delta}{a_0} \quad (1)$$

For elastic materials, a plot of σ_{eng}/E vs δ/a_0 forms a straight line with a slope of 0.85 for both compressive and tensile displacements until the point of detachment of the punch from the layer. From eq 1, it is evident that this relationship remains constant for a given contact radius. Figure 4a shows that the load and displacement are linear during the compressive portion of the stress relaxation test, indicating elastic behavior at small strains in the alginate gels. However, the behavior deviates from this simple relationship as the strain is increased (Figure 5).

Despite the linear stress–strain relationship for an elastic layer in compression and the simplicity of the punch geometry, the stress distribution under the punch is not uniform. In fact, regardless of the degree of elasticity, a stress singularity exists at the edge of contact between a punch and a gel layer.³⁷ Equation 2 describes the normal stress distribution for the frictionless contact of an elastic layer with a flat punch, which is shown in Figure 4b.³⁷

$$\frac{\sigma_{zz}^{\text{adh}}(r)}{\sigma_{\text{eng}}} = \frac{1}{2} \left(1 - \left(\frac{r}{a_0} \right)^2 \right)^{-1/2} \quad (2)$$

This stress distribution is plotted in Figure 4b as a function of r/a_0 , where r is the radial distance from the center of the punch. The increase in stress at the edge of contact results in a local increase in strain in this region, which results in local

relaxation over appropriate time periods for viscoelastic materials. Also in Figure 4b is a schematic displaying the increased stress at the edge of contact for a flat punch and the parameters used in eq 2.

Results

Material Considerations. Because of the ionic nature of alginate hydrogels, several complications can arise during the use and testing of these materials, including swelling, syneresis, and ion exchange. These issues can be influenced by excess, insufficient, or nonuniformly distributed cations in the alginate gels, making the surrounding environment of the hydrogels during storage and testing an important consideration. Additionally, the expulsion of fluid during compression can be an issue for some gels. These material concerns are addressed in this section.

Swelling and syneresis, which have been much addressed in the literature, are not concerns in this work.^{6,7,24,26,30,31} Syneresis is the slow, time-dependent deswelling of a gel that results in the expulsion of liquid, usually during gelation, due to slow ionic cross-linking.^{7,20,30} The gel making procedure used in this work begins with a fairly uniform distribution of calcium ions throughout the alginate solution in the presence of a small concentration of sodium ions, which results in the formation of homogeneous gels.^{16,30,39} It was observed that the thickness of these gels remained constant over long periods of time.

Another interesting study concerns the effect of competing ions on the alginate gel behavior. Draget et al. found that sodium (Na^+) and other monovalent ions have an effect on Ca^{2+} gelation kinetics.²⁹ Like Ca^{2+} , interchain associations with Na^+ are dependent on the guluronic acid content in the alginate.^{24,29} When the two ions are present, there is competition for binding sites in junction zones and ion exchange occurs, even though the affinity for Ca^{2+} is greater.^{24,29} The addition of monovalent salts also affects the mechanical properties of Ca^{2+} alginate gels.^{24,29} The results of LeRoux et al. show a decrease in modulus over time in 0.15 M NaCl solution.²⁴ However, the gels in our experiments experienced little change in mechanical properties after long-term exposure to NaCl. The alginate gel was immersed in an aqueous solution of NaCl (0.14 M) for a total period of 10 days, during which stress relaxation tests were performed on the gel, in NaCl solution, at certain intervals (the NaCl solution was refreshed periodically). Published results indicate that the modulus should decrease and that the gels should eventually disintegrate,^{24,29,31} but in our case, not much change was evident over the 10 day period. This behavior is consistent with the high G content of our gels, which enhances their stability in the presence of monovalent cations; these results make a case for the general robustness of the gels presented in this work.⁶

A final issue to be addressed concerns the possibility of osmotic deswelling of the gels due to stresses applied during the compression experiment. These effects are not a concern for this system because of the time scale of the loading portion of the experiment and because of the relatively low osmotic compressibility of the alginate gels.³⁵

Large Strain Stress Relaxation. The effects of increasing strain magnitude on stress relaxation are displayed in Figure 5. The strain on the alginate gel increases as the maximum compressive displacement is increased from $0.23a_0$ to $4.38a_0$. Additionally, the

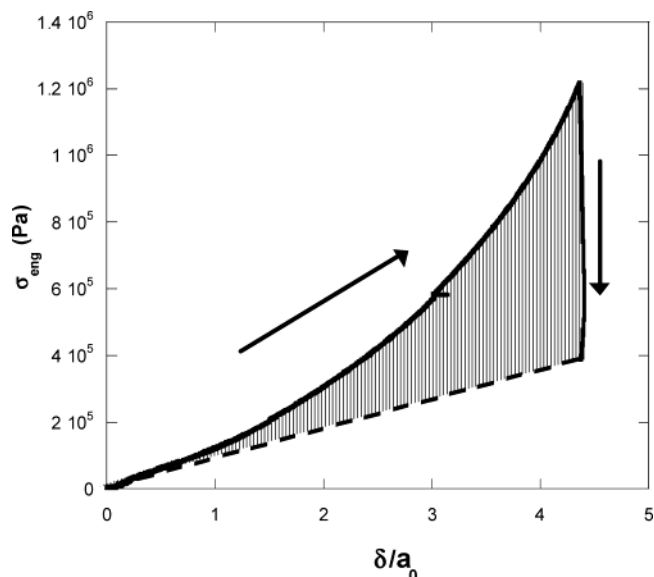


Figure 6. Plot of stress vs normalized displacement from a stress relaxation experiment with a maximum stress of 1.25×10^6 Pa and a δ_{\max} of $4.38a_0$. The data shown represent the behavior during alginate gel compression and relaxation. The dotted line represents the initial, linear load–displacement relationship. The shaded region displays the nonlinear response, which relaxes over time.

maximum stress increases with δ_{\max} . In all cases, the stress decays rapidly to approximately half the maximum value and then decreases more slowly, with the majority of the relaxation taking place within the first several hundred seconds. A plot of load vs displacement for the test conducted with the highest δ_{\max} is shown in Figure 6. The plot shows data from initial contact of the gel, compression to δ_{\max} , and stress relaxation at this fixed value of displacement. The load–displacement relationship is linear for δ/a_0 less than one but increases more rapidly as the strain is increased further. This figure illustrates that the gel relaxes back to the extrapolated linear behavior during the stress relaxation portion of the experiment.

Figure 7 shows the alginate gel modulus as a function of strain magnitude. The relaxed modulus value is given by $E(t')$, where t' is 500 s after the maximum displacement was initially attained, indicated by the arrows on the curves in Figure 5. These moduli are nearly independent of the maximum compressive strain. Moreover, the magnitudes of 10^5 Pa are typical values of small-strain elastic moduli for these alginate hydrogels. The origins of the low moduli for four of the lower strain samples are unknown but are most likely due to an irregularity in those particular samples. Taken together, Figures 5 and 7 indicate that as the maximum strain is increased, stress relaxation becomes more important. The mechanism of stress relaxation most likely involves a de-cross-linking and re-cross-linking of the Ca^{2+} ions.¹⁸ When combined with the strain hardening tendency of the material, the net effect is to obtain a “relaxed” modulus that is roughly independent of δ_{\max}/a_0 .

Dynamic Moduli at Intermediate Strains. Figure 8 shows the load and displacement data from a typical relaxed sine wave experiment with an initial compressive δ_{\max} of $0.38a_0$ and a displacement amplitude (δ_0) of $80 \mu\text{m}$ at 0.01 Hz. After the stress relaxation portion of the experiment, the displacement oscillates (Figure 8b) while the load response follows this movement (Figure 8a). Figure 8c shows the load–displacement

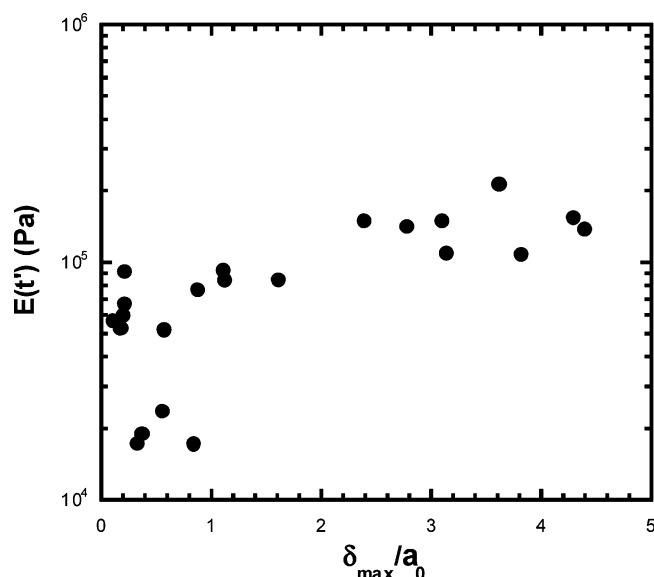


Figure 7. Modulus as a function of strain from stress relaxation experiments. $E(t')$ is the modulus value at time t' , 500 s after the time at which δ_{\max} was attained.

relationship for the stress relaxation and first sine wave frequency portions of the experiment. The cyclic nature of the test is apparent. In this case, the indenter remained in complete contact with the gel, such that $\delta(t)$ and the load response $P(t)$ are both sinusoidal.

The storage and loss moduli at each frequency are calculated by measuring the phase angle, Δ , between the applied displacement and resulting force. At each frequency, the complex modulus is measured as³⁶

$$E^* = \frac{3P_0}{8a_0\delta_0} \quad (3)$$

The storage (E') and loss (E'') moduli are related to E^* by the following:

$$E' = E^* \cos \Delta \quad (4)$$

$$E'' = E^* \sin \Delta \quad (5)$$

The storage and loss moduli (E' and E'') as functions of frequency from a relaxed sine wave experiment are shown in Figure 9 for $\delta_0 = 80 \mu\text{m}$. The elastic character of the gel is evident by the fact that E' exceeds E'' and is not strongly dependent on the frequency. This result is consistent with both the high concentration of Ca^{2+} used to form the gel and the high G content of the alginate.¹⁸

Adhesion. As displayed in Figure 10 for a test with $\delta_{\max} = 0.21a_0$ and $\delta_0 = 160 \mu\text{m}$, adhesion is insufficient to maintain contact for large displacement amplitudes. During the first cycle (arrows B–C in Figure 10c), the punch detaches from the gel when the tensile load reaches 4.6 mN, causing a flattening of the load signal as it drops to zero (Figure 10a). The displacement remains sinusoidal (Figure 10b) because the waveform of the applied displacement (input) is not changed. Figure 10c displays the new load–displacement relationship for this experiment with arrows giving the progression of the test. Arrows A and A' show the stress relaxation portion of the test while arrows B–C and D–E represent the first sine wave cycle and subsequent sine wave cycles, respectively.

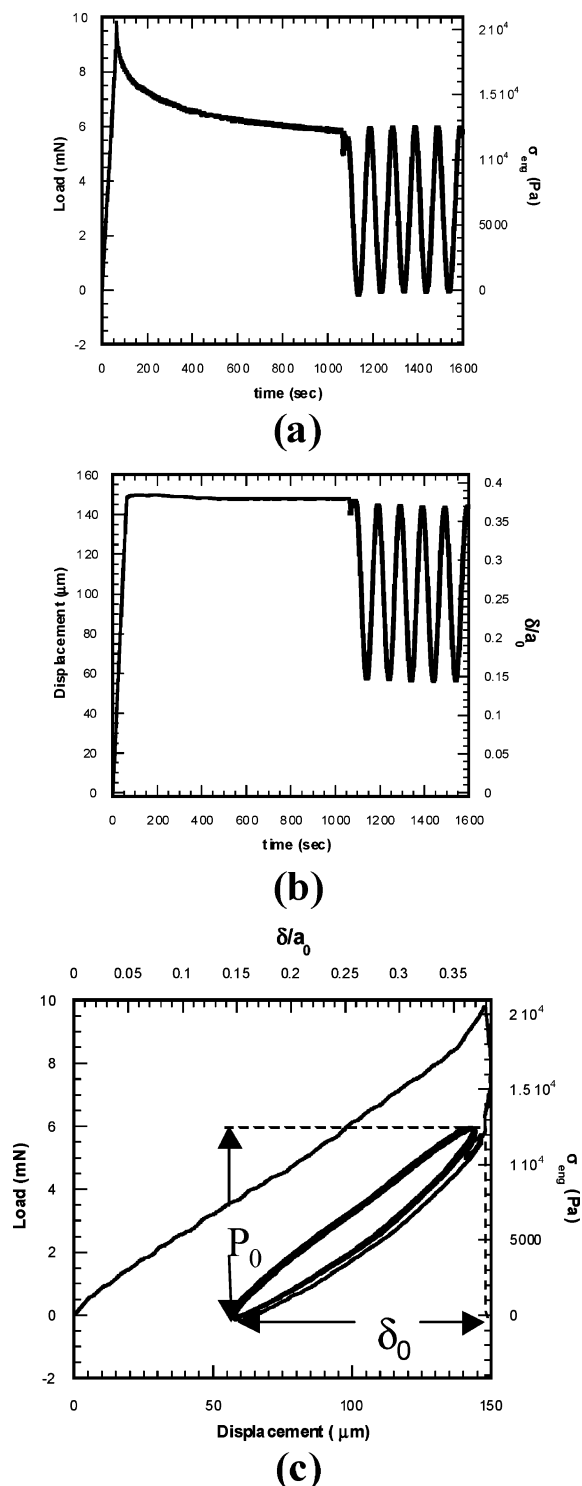


Figure 8. (a) Load as a function of time, (b) displacement as a function of time, and (c) the load–displacement relationship during a typical relaxed sine wave test. P_0 and δ_0 represent the load and displacement amplitudes, respectively, of the sine wave oscillation.

Time-dependent adhesion is evident in the behavior shown in Figure 10a. Prior to the first tensile cycle of the sine wave experiment, the punch has remained in contact with the gel for the entire relaxation portion of the experiment, which lasted for approximately 1000 s. After the punch detaches from the gel at a critical load of 4.6 mN, it is subsequently brought into contact and then detached again during each cycle, remaining in contact with the gel for a much shorter period of time.

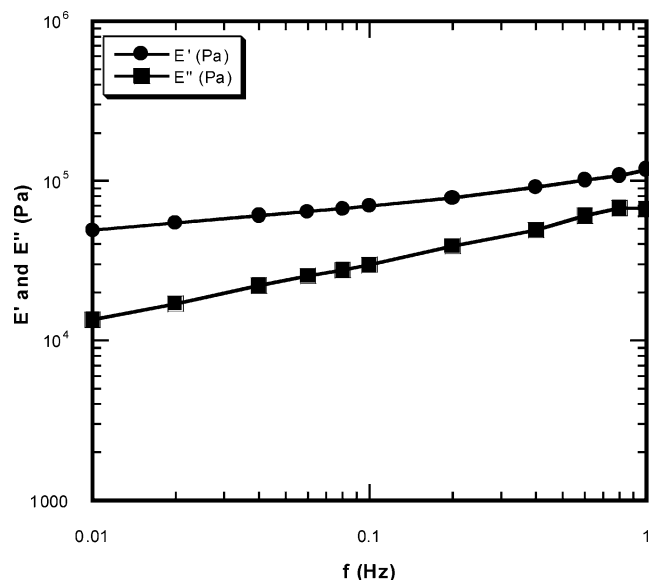


Figure 9. Storage and loss moduli as functions of frequency from oscillatory experiments ($\delta_0 = 80 \mu\text{m}$).

As a result, the tensile load required to remove the punch from the gel during subsequent cycles is much smaller, equal to about 0.4 mN. We attribute this result to the fact that the adhesive interactions between the punch and gel depend on the contact time.

The adhesive interactions can be quantified by calculating the energy release rate, \mathcal{G} , characterizing the driving force for adhesive failure at the gel/punch interface. The energy release rate is related to the tensile load, P_t , by the following expression:³⁷

$$\mathcal{G} = \frac{3}{32\pi} \frac{P_t^2}{Ea_0^3} \quad (6)$$

Failure occurs when \mathcal{G} exceeds the critical energy release rate, \mathcal{G}_c , which can be obtained by using the maximum tensile load for P_t in eq 6. From this, we obtain $\mathcal{G}_c = 106 \text{ mJ/m}^2$ for the first cycle and $\mathcal{G}_c = 0.8 \text{ mJ/m}^2$ for subsequent cycles.

The time dependence of the development of adhesive contact between the punch and the gel is most likely related to aging effects that have also been observed during frictional studies of polymer gels.⁴⁰ While a detailed investigation of these interactions is beyond the scope of this work, it is clear that the weak adhesion observed for short contact times limits our ability to conduct oscillatory tests at large strain amplitudes. In the absence of substantial adhesion between the punch and the gel, it is important to remain in a state of compression at all times. This requirement is further complicated by creep effects that are discussed in more detail in the following section.

Nonrecoverable Creep. A series of stress relaxation tests to determine the extent of permanent deformation of the alginate gels were also performed. These tests consisted of a typical stress relaxation experiment with δ_{max} of 174, 440, 1090, or 1415 μm , followed by load relaxation for 2000 s. After relaxation, the punch was retracted from the gel until complete detachment and then pushed back into the gel in the same place until contact was reinitiated. This allowed determination of the difference between zero displacement at initial contact for a nondeformed sample and the displacement

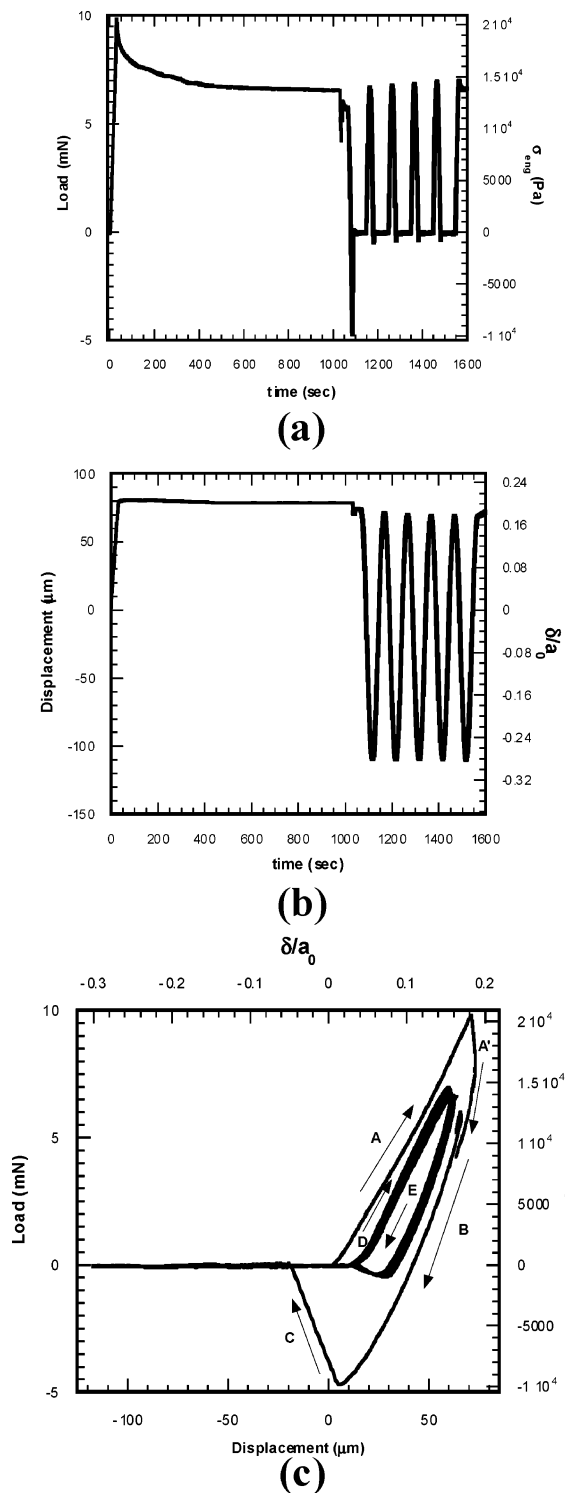


Figure 10. (a) Load as a function of time, (b) displacement as a function of time, and (c) the load–displacement relationship during a typical relaxed sine wave test during which the punch came out of contact with the gel. Arrows and letters show the progression of punch movement.

to reach contact with the gel again after indentation and detachment. A displacement greater than zero describes the extent of permanent deformation. Figure 11 displays the results of these tests in terms of the displacement necessary to reinstate contact (δ_{plastic}) after the punch had detached from the stress relaxation test. The permanent deformation increases with applied strain as expected. The punch leaves an indentation in the gel, and as a result, more forward displacement is required

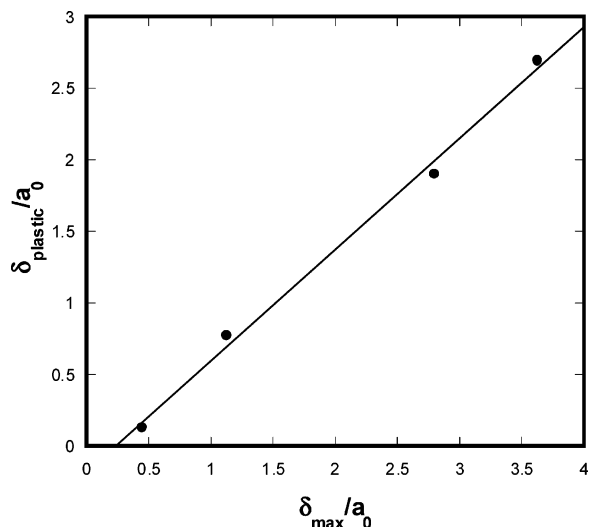


Figure 11. Normalized displacement required to reinitiate contact in an alginate gel after imposing an initial compressive displacement of δ_{\max} and retracting the indenter. The solid black line is a linear fit to the data (eq 7).

to reinitiate contact for the second test. The equation for the linear fit shown in Figure 11 is

$$\frac{\delta_{\text{plastic}}}{a_0} = -0.18 + 0.78 \frac{\delta_{\max}}{a_0} \quad (7)$$

Extrapolation of this line through the x -axis yields δ_{\max}/a_0 of approximately 0.23, which is the strain value under which no permanent deformation will occur. This magnitude is typical of strain amplitudes used in oscillatory tests, a result that is consistent with the largely elastic behavior of the gels at these low strains.

Discussion

The results of these tests display the dual nature of transient networks, with elastic behavior at small strains giving way to viscoelasticity at higher strain magnitudes. Insight into the elusive nature of these systems can be gleaned from recent studies to explore a means to increase both the elastic modulus and the toughness of alginate hydrogels.¹⁸ Kong et al. propose that ionic cross-links in alginate hydrogels dissipate deformation energy via a partial, stepwise de-cross-linking.¹⁸ This sequential energy dissipation suppresses complete, catastrophic de-cross-linking of all the G blocks and creates an effectively larger plastic zone during deformation.¹⁸ Ionic cross-links are quite effective at energy dissipation, such that the work to fracture a covalently cross-linked alginate gel is 2 orders of magnitude lower than that for ionically cross-linked alginate gels.¹⁸ The strain magnitude-dependent storage modulus of the ionic gels allows additional deformation and plasticity beyond covalent gels. Although ionic alginate gels behave viscoelastically, increasing the concentration of the ionic cross-linker (Ca^{2+}) can reduce the frequency dependence of the storage modulus, resulting in nearly elastic behavior. The threshold for gelation in the gels investigated by Kong et al. is 0.24 mol/mol of Ca^{2+} to alginate, whereas the mole fraction used for our gels is 0.49 mol/mol.¹⁸ The larger mole fraction used in our studies produces stiffer alginate gels (10^5 Pa compared to 10^4 Pa). This enhancement is due not only to increased cross-linking from a larger number of available calcium ions but also to slightly different

alginate copolymer compositions; i.e., our alginate material had more or longer G-blocks.^{18,20} Kong et al. found that ionic gels with high ionic cross-linking density behave as elastic solids at small deformations and have a capacity to dissipate energy at larger deformations.¹⁸ Their conclusions and findings for alginate hydrogels in shear and notched tension are in qualitative agreement with the results of this independent study of hydrogels in compression.

Although the techniques described in this paper are very useful in investigating high strain–stress relaxation behavior in alginate hydrogels, the combination of creep behavior and weak adhesion in these materials limits the practical use of the oscillatory tests. The maximum δ_0 that we can impose is restricted by both \mathcal{G}_c and the plastic flow of the material. We can begin to quantify the degree of this limitation by considering the criterion for detachment of a thick elastic layer from a flat punch during tensile movement. Equations 1 and 6 can be combined to obtain the following expression:³⁵

$$\frac{\delta^*}{a_0} = \left(\frac{3\pi}{2} \right)^{1/2} \left(\frac{\mathcal{G}_c}{Ea_0} \right)^{1/2} \quad (8)$$

where δ^* is the tensile displacement at which detachment occurs, i.e., $\mathcal{G} = \mathcal{G}_c$ when $\delta = \delta^*$. From eq 8, we can calculate the allowable δ^*/a_0 for the situation shown in Figures 10, using $E = 10^5$ Pa and the values of \mathcal{G}_c determined earlier. For the first cycle, $\mathcal{G}_c = 106$ and $\delta^*/a_0 = 0.11$. For subsequent cycles, $\mathcal{G}_c = 0.8$ mJ/m² and $\delta^*/a_0 = 0.01$. The pulloff displacement is defined with respect to the displacement where the load is equal to zero. This reference displacement is moved into the sample by plastic deformation at high compressive strains, thereby introducing an important practical limitation on the displacement amplitude that can be used in the oscillatory experiments.

Summary

We have explored the time-dependent mechanical behavior of alginate hydrogels, using a novel test method developed for these types of materials. Our tests used a flat probe geometry, where δ/a_0 (compressive punch displacement normalized by punch radius) gives a measure of the overall strain applied to the system. Alginate hydrogels are dually elastic and viscoelastic materials, depending on the strain amplitude. For $\delta/a_0 < 0.25$, the alginate gels behave elastically, with little nonrecoverable creep and with dynamic moduli that are only weakly frequency dependent. Our ability to investigate large values of δ/a_0 in a dynamic oscillatory experiment was limited by the adhesion of the gel to the probe, which was found to be strongly dependent on the contact time. The time-dependent behavior at these large strains was investigated by compressive stress relaxation experiments. An enhanced stress relaxation observed at large strains, combined with the strain hardening behavior of the material, gives an effective “relaxed” elastic modulus that is nearly independent of δ/a_0 . The ability of the material to relax large stresses, such as those characterized by the stress concentration at the probe edge or at a crack tip, is responsible for the large mechanical toughness of these materials.

Acknowledgment. This work was supported by the National Science Foundation under Grant DMR-0214146.

The authors acknowledge Dr. Lonnie Shea's group at Northwestern University, particularly Pam Kreeger, for helpful information regarding alginate gels and for donating the alginate material used in these studies.

References and Notes

- (1) Hotta, A.; Clarke, S. M.; Terentjev, E. M. *Macromolecules* **2002**, *35*, 271.
- (2) Filali, M.; Ouazzani, M. J.; Michel, E.; Aznar, R.; Porte, G.; Appell, J. *J. Phys. Chem. B* **2001**, *105*, 10528.
- (3) Vlassopoulos, D.; Pitsikalis, M.; Hadjichristidis, N. *Macromolecules* **2000**, *33*, 9740.
- (4) Eiselt, P.; Yeh, J.; Latvala, R. K.; Shea, L. D.; Mooney, D. J. *Biomaterials* **2000**, *21*, 1921.
- (5) Jeong, B.; Bae, Y. H.; Lee, D. S.; Kim, S. W. *Nature (London)* **1997**, *388*, 860.
- (6) Martinsen, A.; Skjakbraek, G.; Smidsrod, O. *Biotechnol. Bioeng.* **1989**, *33*, 79.
- (7) Draget, K. I.; Gaserod, O.; Aune, I.; Andersen, P. O.; Storbakken, B.; Stokke, B. T.; Smidsrod, O. *Food Hydrocolloids* **2001**, *15*, 485.
- (8) Smidsrod, O.; Skjakbraek, G. *Trends Biotechnol.* **1990**, *8*, 71.
- (9) Lim, F.; Sun, A. M. *Science* **1980**, *210*, 908.
- (10) Nowak, A. P.; Breedveld, V.; Pakstis, L.; Ozbas, B.; Pine, D. J.; Pochan, D.; Deming, T. J. *Nature (London)* **2002**, *417*, 424.
- (11) Joly-Duhamel, C.; Hellio, D.; Djabourov, M. *Langmuir* **2002**, *18*, 7208.
- (12) Joly-Duhamel, C.; Hellio, D.; Ajdari, A.; Djabourov, M. *Langmuir* **2002**, *18*, 7158.
- (13) Gombotz, W. R.; Wee, S. F. *Adv. Drug Delivery Rev.* **1998**, *31*, 267.
- (14) Kreeger, P. K.; Woodruff, T. K.; Shea, L. D. *Mol. Cell. Endocrinol.* **2003**, *205*, 1.
- (15) Rowley, J. A.; Madlambayan, G.; Mooney, D. J. *Biomaterials* **1999**, *20*, 45.
- (16) Moe, S. T.; Draget, K. I.; Skjak-Braek, G.; Smidsrod, O. In *Food Polysaccharides and Their Applications*; Stephen, A. M., Ed.; Marcel Dekker: New York, 1995; Vol. 67, p 245.
- (17) Grant, G. T.; Morris, E. R.; Rees, D. A.; Smith, P. J. C.; Thom, D. *FEBS Lett.* **1973**, *32*, 195.
- (18) Kong, H. J.; Wong, E.; Mooney, D. J. *Macromolecules* **2003**, *36*, 4582.
- (19) Stokke, B. T.; Smidsrod, O.; Buheim, P.; Skjakbraek, G. *Macromolecules* **1991**, *24*, 4637.
- (20) Stokke, B. T.; Draget, K. I.; Smidsrod, O.; Yuguchi, Y.; Urakawa, H.; Kajiwara, K. *Macromolecules* **2000**, *33*, 1853.
- (21) Rees, D. A. *Pure Appl. Chem.* **1981**, *53*, 1.
- (22) Moe, S. T.; Draget, K. I.; Skjakbraek, G.; Smidsrod, O. *Carbohydr. Polym.* **1992**, *19*, 279.
- (23) Matsumoto, M.; Ohashi, K. *Biochem. Eng. J.* **2003**, *14*, 75.
- (24) LeRoux, M. A.; Guilak, F.; Setton, L. A. *J. Biomed. Mater. Res.* **1999**, *47*, 46.
- (25) Gaserod, O.; Smidsrod, O.; Skjak-Braek, G. *Biomaterials* **1998**, *19*, 1815.
- (26) Draget, K. I.; Ostgaard, K.; Smidsrod, O. *Carbohydr. Polym.* **1991**, *14*, 159.
- (27) Zheng, H. H. *Carbohydr. Res.* **1997**, *302*, 97.
- (28) Andresen, I. L.; Smidsrod, O. *Carbohydr. Res.* **1977**, *58*, 271.
- (29) Draget, K. I.; Steinsvag, K.; Onsoyen, E.; Smidsrod, O. *Carbohydr. Polym.* **1998**, *35*, 1.
- (30) Velings, N. M.; Mestdag, M. M. *Polym. Gels Networks* **1995**, *3*, 311.
- (31) Segeren, A. J. M.; Boskamp, J. V.; van den Temple, M. *Faraday Discuss.* **1974**, *57*, 255.
- (32) Foros, H. February 23, 2004.
- (33) Ahn, D.; Shull, K. R. *Macromolecules* **1996**, *29*, 4381.
- (34) Shull, K. R.; Ahn, D.; Chen, W. L.; Flanigan, C. M.; Crosby, A. J. *Macromol. Chem. Phys.* **1998**, *199*, 489.
- (35) Webber, R. E.; Shull, K. R.; Roos, A.; Creton, C. *Phys. Rev. E* **2003**, *68*.
- (36) Crosby, A. J.; Shull, K. R.; Lin, Y. Y.; Hui, C. Y. *J. Rheol.* **2002**, *46*, 273.
- (37) Shull, K. R. *Mater. Sci. Eng. R* **2002**, *36*, 1.
- (38) Shull, K. R.; Flanigan, C. M.; Crosby, A. J. *Phys. Rev. Lett.* **2000**, *84*, 3057.
- (39) Skjakbraek, G.; Grasdalen, H.; Smidsrod, O. *Carbohydr. Polym.* **1989**, *10*, 31.
- (40) Baumberger, T.; Caroli, C.; Ronsin, O. *Eur. Phys. J. E* **2003**, *11*, 85.

MA049274N